Journal of Biomolecular NMR, **18:** 269–277, 2000.
KLUWER/ESCOM

Studies of physicochemical properties of N-H• • •N hydrogen bonds in DNA, using selective ^{15}N-labeling and direct ^{15}N 1D NMR

Chojiro Kojima[a], Akira Ono[b] & Masatsune Kainosho[a,b,*]
[a]*CREST (Core Research Evolutional Science and Technology), Japan Science and Technology Corporation (JST), Kawaguchi, Saitama 332-0012, Japan*
[b]*Department of Chemistry, Faculty of Science, Tokyo Metropolitan University, Hachioji, Tokyo 192-0397, Japan*

Received 14 June 2000; Accepted 18 September 2000

Key words: DNA oligomer, hydrogen exchange, nitrogen-nitrogen J coupling constant, scalar coupling constants across hydrogen bonds, temperature dependence

Abstract

^{15}N-^{15}N scalar coupling constants across base pair hydrogen bonds ($^{2h}J_{NN}$) were studied using residue- and atom-specifically ^{15}N labeled DNA oligomers. The N3 atom selectively ^{15}N enriched 2′-deoxycytidine and thymidine, and the uniformly ^{15}N enriched 2′-deoxyadenosine and 2′-deoxyguanosine, were chemically prepared and incorporated into two DNA oligomers, d(CGCGAATTCGCG)$_2$ and d(CGCAAAAAGCG)•d(CGCTTTTTGCG). This isotope labeling enabled us to determine the $^{2h}J_{NN}$ value from the splitting of the ^{15}N 1D spectrum. Additionally, it enabled the determination of $^{2h}J_{NN}$ in D_2O quite easily and highly quantitatively. The temperature and DNA sequence dependence were examined for these oligomers. The sequence dependence was not clear; however, a significant decrease of $^{2h}J_{NN}$ was observed by elevating the temperature. This temperature dependence was not due to the hydrogen exchange, since the addition of 20 mM NH_3 did not change the $^{2h}J_{NN}$ values. The $^{2h}J_{NN}$ values in D_2O were somewhat smaller than those in H_2O. As compared to our ^{15}N 1D method, the quantitative HNN-COSY method gave systematically smaller $^{2h}J_{NN}$ values in our system, due to the lower ^{15}N fraction of our sample (79 and 88% for dA and the other nucleotides, respectively) and the insufficient power of the ^{15}N RF pulse ($B_1 = 6.6$ kHz). These systematic differences were recovered by theoretical correction of the ^{15}N isotope fraction contribution, by using the composite ^{15}N 180° pulse in a quantitative HNN-COSY experiment.

Introduction

NMR scalar coupling constants across hydrogen bonds have been discovered and quantitatively determined for both nucleic acids (Dingley and Grzesiek, 1998; Pervushin et al., 1998) and proteins (Cordier and Grzesiek, 1999; Cornilescu et al., 1999; Hennig and Geierstanger, 1999). Theoretical quantum-chemical calculations have indicated that these J-coupling constants are dominated by the Fermi contact term, like the common J-coupling constants through covalent bonds (Dingley et al., 1999; Scheurer and Brüschweiler, 1999). These J-coupling constants are roughly proportional to the amide- and imino-proton chemical shifts (Cordier and Grzesiek, 1999; Dingley et al., 1999; Scheurer and Brüschweiler, 1999). The strength of the hydrogen bond is related to the proton chemical shifts (Hibbert and Emsley, 1990); thus, the J-coupling constants across hydrogen bonds are expected to be related to the hydrogen bond strength. However, thus far no clear relation has been obtained between the J-coupling constants and the hydrogen bond strength. In order to make such a relationship clear, the physicochemical properties of the observed J-coupling constants need to be investigated.

The J-couplings across hydrogen bonds have been studied for DNA and RNA oligomers with Watson–Crick type and the other unusual base pairs (Dingley and Grzesiek, 1998; Pervushin et al., 1998; Dingley

*To whom correspondence should be addressed. E-mail: kainosho@nmr.chem.metro-u.ac.jp

et al., 1999, 2000; Majumdar et al., 1999a, b; Wöhnert et al., 1999; Hennig and Williamson, 2000; Liu et al., 2000). For Watson–Crick base paired DNA, Pervushin et al. have reported the scalar coupling constants across hydrogen bonds (Pervushin et al., 1998), which are the homonuclear ^{15}N-^{15}N couplings ($^{2h}J_{NN}$) and the heteronuclear ^{1}H-^{15}N couplings ($^{1h}J_{NH}$). The determined values ranged from 6.0 to 7.0 Hz ($^{2h}J_{NN}$) and 1.8 to 3.6 Hz ($^{1h}J_{NH}$) with 0.1 Hz and 0.1 to 0.6 Hz errors, respectively (see Table 1 of Pervushin et al., 1998). Pervushin et al. measured the splitting of $^{h}J_{NN}$-correlation-[^{1}H, ^{15}N]-TROSY and [^{1}H, ^{15}N]-TROSY for $^{1h}J_{NH}$ and $^{2h}J_{NN}$, respectively. Generally, the scalar coupling constants do not depend on the determination method, and thus other techniques, including quantitative J_{NN} HNN-COSY experiments, will give identical results.

The direct reading of ^{15}N splitting of a 1D spectrum is one of the most straightforward methods to determine the scalar coupling constants across the hydrogen bond ($^{2h}J_{NN}$) value. However, the presence of the homonuclear ^{15}N-^{15}N coupling constants within the base ring makes it difficult to determine the $^{2h}J_{NN}$ value from the splitting of the ^{15}N resonance. Some homonuclear ^{15}N-^{15}N coupling constants of AMP, GMP, CMP, and UMP have been determined previously (Levy and Lichter, 1979; Ono, 1997), and they are less than 6 Hz and smaller than the $^{2h}J_{NN}$ values. Due to the limitation of the ^{15}N linewidth of a DNA oligomer, no clear splitting from such small coupling constants is seen, and the apparent signal just becomes broad. This broadening causes sensitivity loss and may hide the scalar couplings across the hydrogen bond, which have not been observed for a long time. The ^{15}N homonuclear selective decoupling can be used to remove this broadening, although it is technically difficult to obtain a high quality spectrum. However, our alternative procedure, atom-selective ^{15}N enrichment, is simpler and easier.

We have prepared pyrimidine N3-site selectively ^{15}N enriched DNA oligomers to study the scalar coupling constants across the hydrogen bond ($^{2h}J_{NN}$). This isotope labeling enables us to determine the $^{2h}J_{NN}$ value from the splitting of the ^{15}N 1D spectrum. Using this technique, the following were examined: the temperature dependence, the magnetic field dependence, the DNA sequence dependence, the solvent dependence, and the basic catalysis [NH_3] effect. The J-coupling constant obtained from the splitting of the ^{15}N 1D spectrum is compared with that from a quantitative HNN-COSY experiment.

Materials and Methods

DNA chemical synthesis. The ^{15}N enriched deoxynucleotides, [$^{15}N_5$]-2′-deoxyadenosine (dA), [$^{15}N_5$]-2′-deoxyguanosine (dG), [3-^{15}N]-2′-deoxycytidine (dC), and [3-^{15}N]-thymidine (T), were synthesized (Ono et al., 1994; Ariza et al., 1995). The ^{15}N labeling efficiency was estimated to be 79% for dA and 88% for dG, dC, and T from ^{1}H 1D NMR. The 3′-phosphoramidite derivatives of each nucleotide were used for DNA oligonucleotide synthesis on a DNA synthesizer (Applied Biosystems Inc., ABI model 392). The synthesized sequences were d(CGC**GA**AT**TC**GCG), d(CGC**A**AAAAGCG), d(CG CTTTT**T**GCG), d(CGCAA**A**AAGCG), and d(CGC TT**T**TTGCG), where bold letters indicate the ^{15}N enriched nucleotides. These oligomers were purified by HPLC using C18 and gel-filtration columns. The details of the purification procedure were published previously (Kyogoku et al., 1995). The 1:1 stoichiometry in duplex formation was adjusted by using the absorptivity at 260 nm. The sequence d(CGCGAATTCGCG) was self-complementary, and thus the duplex was formed by annealing under NMR buffer conditions. The prepared duplexes were named as follows: d(CGC**GA**AT**TC**GCG)$_2$ = D12, d(CGC**A**AAAAGCG) • d(CGCTTTT**T**GCG) = AT11-t, and d(CGCAA**A**AAGCG) • d(CGCTT**T**TTG CG) = AT11-c.

Sample preparation. All NMR samples were dissolved in 250 μl of 10 mM phosphate buffer (pH 6.8) containing 100 mM NaCl and 0.1 mM EDTA, lyophilized, and dissolved in 90% H_2O / 10% D_2O. The D_2O sample was prepared by lyophilizing the H_2O sample and dissolving it in 90% D_2O / 10% H_2O. The resulting solution was kept in a 5 mm micro tube (Shigemi Co., Tokyo). The double-strand concentrations were about 2, 2, and 3 mM for the AT11-t, AT11-c, and D12 samples, respectively. For the basic catalysis NH_3 concentration dependence experiments, the pH of the D12 sample was re-adjusted to 8.7.

NMR measurements. The NMR spectra were obtained using Bruker DRX600 and DRX800 spectrometers operating at 600 and 800 MHz ^{1}H frequencies, respectively. The ^{15}N 1D spectra with ^{1}H or ^{2}H decoupling were measured on the DRX800 or DRX600 spectrometer at 10, 20, 35, and 50 °C for D12, and at 10, 20, and 40 °C for the AT11-t and AT11-c samples. For each spectrum, 16K, 32K, or 64K scans

were accumulated for 0.5, 1, or 2 days of measurement, respectively, in order to yield signal-to-noise ratios greater than 8, which ensures that the expected errors would be less than ± 0.2 Hz. The number of scans was determined from the signal-to-noise ratio. The quantitative HNN-COSY spectra were measured on the DRX600 at 2, 5, 10, 15, 20, 25, 30, 35, 40, 45, and 50 °C for D12. Each quantitative HNN-COSY experiment took 1 day for D12, using the parameters in the original report (e.g. ^{15}N carrier frequency at 185 ppm) (Dingley and Grzesiek, 1998), except that the ^{15}N to ^{15}N coherence transfer delay time was 20 ms, the RF power for the ^{15}N high power pulse was 6.6 kHz, and the t_1 column contained either 512 or 1024 complex points. To estimate the experimental error of the determined $^{2h}J_{NN}$, four delay times, 7.5, 15, 22.5, and 30 ms, were used at 20 °C for D12 on the DRX600. To see the hydrogen exchange effect, the ^{15}N 1D spectra and the quantitative HNN-COSY spectra were measured on the DRX800 and DRX600 spectrometers, respectively, at 10, 20, and 40 °C with an ammonium ion concentration of 20 mM at pH 8.7.

Results

The ^{15}N 1D spectrum of the D12 sample is shown in Figure 1. The assignments are given in the top spectrum (a) of Figure 1, and the expanded spectra of the N3 signals of 2′-deoxycytidine (b) and thymidine (c) are shown at the bottom. The splitting pattern was complex, although it was expected to be a doublet due to the relatively large $^{2h}J_{NN}$ value and the selective ^{15}N enrichment at the N3 position. This apparent difference comes from the lower fraction of ^{15}N enrichment, 79% for dA and 88% for dG, although the ^{15}N fractions of T and dC did not affect their own splitting patterns. When the ^{15}N fractions of dA and dG were less than 100%, the center peak was seen on the N3 signals of T and dC. Even for this simple doublet system, the ^{15}N splitting pattern was seriously affected by the ^{15}N fraction of the base paired nitrogen. In our case, the intensity of the center peak was estimated to be about 53 and 27% of the main doublet peaks for T and dC, respectively. These center peaks were not detected by the two-dimensional ^{1}H-^{15}N correlation method of HSQC and TROSY (data not shown). For dA and dG, the splitting of the N1 signal caused by the hydrogen bonding was not observed, since the lower ^{15}N fraction resulted in a complicated splitting pattern that obscured this splitting. Although the percentages of the ^{15}N enrichment, 79 and 88%, were sufficient to see the signals, the resultant $^{2h}J_{NN}$ values were seriously affected by these small imperfections.

Table 1. Magnetic field dependence of ^{15}N-^{15}N J-coupling across the hydrogen bond[a]

Magnetic field strength (T)	Coupling at a temperature of			
	10 °C	20 °C	35 °C	50 °C
14.1	7.2	7.0	6.9	
18.8	7.4	6.8	6.8	6.7

[a] $^{2h}J_{NN}$ (in Hz) between 5A:N1 and 8T:N3 of d(CGCG**A**AT**T**CGCG)$_2$ in H_2O obtained from the ^{15}N 1D splitting. Experimental error ± 0.2 Hz.

The $^{2h}J_{NN}$ value was determined by reading the splitting of the ^{15}N 1D spectrum, using the line shape fitting tool of the FELIX software and taking into account the center peak contribution. The experimental error, ± 0.2 Hz, was estimated by repeating the same experiments two to four times with different scan and processing parameters, and was defined as the maximum difference of the determined $^{2h}J_{NN}$ values. Three or four different temperatures between 10 and 50 °C were used to study the temperature dependence of $^{2h}J_{NN}$ and to assess the other physical properties, as shown below. First, the magnetic field dependence of $^{2h}J_{NN}$ was examined, as shown in Table 1. At three temperatures, 10, 20, and 35 °C, no difference of the $^{2h}J_{NN}$ values was found between the 14.1 and 18.8 T magnetic fields (600 and 800 MHz ^{1}H frequency) within the experimental error, ± 0.2 Hz. This means that the observed $^{2h}J_{NN}$ value was primarily due to the scalar interaction and not the cross-correlated relaxation contribution. These results are consistent with the previous reports (Dingley and Grzesiek, 1998; Pervushin et al., 1998).

Second, the DNA sequence dependence of $^{2h}J_{NN}$ is shown in Table 2. Two DNA sequences were employed for this purpose, where one was the typical B-family DNA dodecamer and the other was the A-tract 'bent' DNA undecamer. In Table 2, the ^{15}N enriched residues are shown by bold letters. For the A-tract sequence, two different sites were independently ^{15}N enriched where the base-pair lifetimes were drastically different, i.e., 57 and less than 3 ms for the center and the 5′ side of the A-tract, respectively (Leroy et al., 1988). A comparison of the three sequences revealed no clear difference at 10 and 20 °C. However, at 40 °C, the $^{2h}J_{NN}$ value of the third sequence in Table 2 was larger than that of the second.

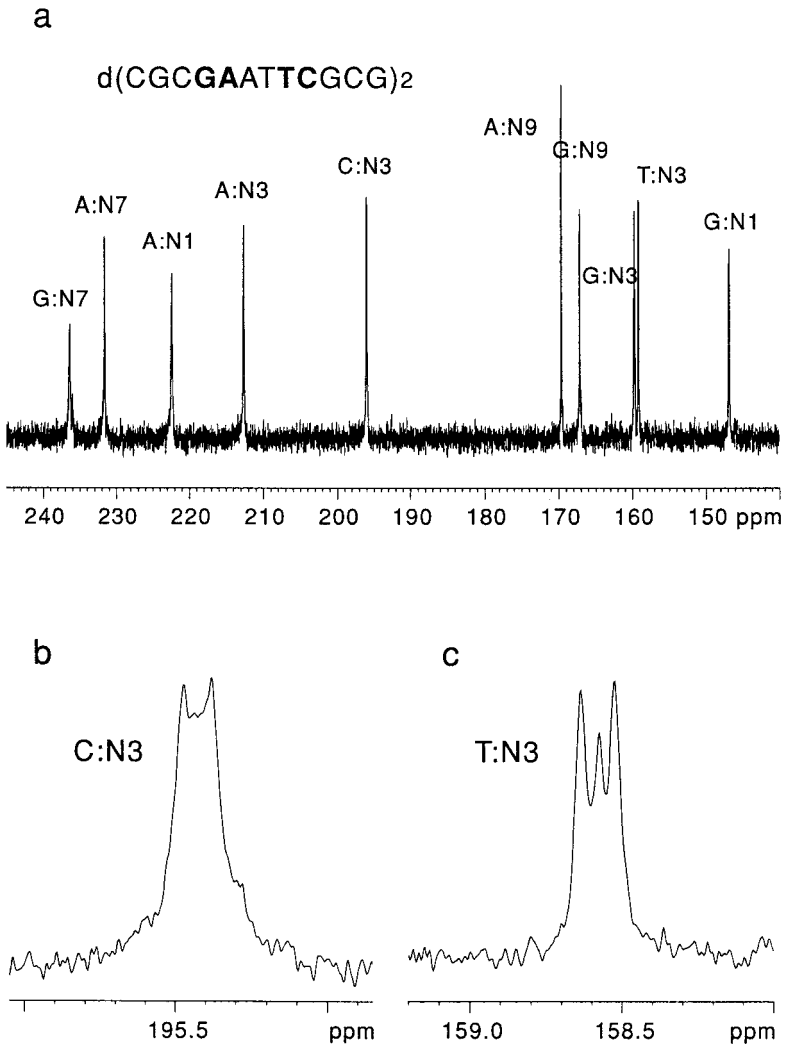

Figure 1. ^{15}N 1D spectrum of a DNA dodecamer recorded at 18.8 T at 20 °C with ^{1}H decoupling ($B_1 = 3.3$ kHz), whole spectrum (a), and expanded spectra of the N3 signals of dC (b) and T (c). The DNA sequence is d(CGC**GA**AT**TC**GCG)$_2$, where the bold letters are the ^{15}N enriched residues. Purine nucleotides are uniformly ^{15}N enriched, and pyrimidine nucleotides are selectively ^{15}N enriched at the N3 position. The ^{15}N fractions are 79 and 88% for dA and the other nucleotides, respectively.

Table 2. Sequence dependence of ^{15}N-^{15}N J-couplings across the hydrogen bond[a]

DNA sequence	Coupling at a temperature of				
	10 °C	20 °C	35 °C	40 °C	50 °C
d(CGCG**A**AT**T**CGCG)$_2$	7.4	6.8	6.8		6.7
d(CGC**A**AAAAGCG) • d(CGCTTTTT**T**GCG)	7.4	6.9		6.6	
d(CGCAA**A**AAGCG) • d(CGCTTT**T**TGCG)	7.6	7.1		7.0	

[a] $^{2h}J_{NN}$ (in Hz) between A:N1 and T:N3 in H_2O at 18.8 T obtained from the ^{15}N 1D splitting. Experimental error ± 0.2 Hz.

Table 3. Solvent dependence of ^{15}N-^{15}N J-couplings across the hydrogen bond[a]

Solvent	Coupling at a temperature of		
	10 °C	20 °C	35 °C
H_2O	7.2	7.0	6.9
D_2O	6.8	6.7	6.5

[a] $^{2h}J_{NN}$ (in Hz) between 5A:N1 and 8T:N3 of d(CGCG**A**AT**T**CGCG)$_2$ at 14.1 T obtained from the ^{15}N 1D splitting. Experimental error ± 0.2 Hz.

This may be due to a difference in the base pair stability, as seen for each end of DNA triplex strands (Dingley et al., 1999).

Third, the solvent dependence of $^{2h}J_{NN}$ is shown in Table 3. In D_2O, the $^{2h}J_{NN}$ values were 0.3–0.4 Hz smaller than those in H_2O at three temperatures, 10, 20, and 35 °C. Although the differences were rather small, they were systematic. The geometric H/D isotope effects appear in both the hydrogen and the heavy atom positions: the N–H bond length is longer than that of the N–D bond, and the heavy atom distance increases by deuteration (Hibbert and Emsley, 1990; Benedict et al., 1998). These geometric changes tend to decrease the $^{2h}J_{NN}$ value. To understand the quantitative relationship between them, a more careful investigation, including theoretical calculations, will be required. The deuteron contribution to the apparent ^{15}N splitting at three experimental conditions is shown in Figure 2. The left (a–c) and right (d–f) spectra show the N3 signals of cytidine and thymidine, respectively. The top spectra (a, d) were measured in H_2O, and the middle (b, e) and bottom (c, f) ones were in D_2O without and with deuterium decoupling, respectively. Without deuterium decoupling, the ^{15}N signals were broadened due to scalar relaxation and the presence of $^{1h}J_{DN}$ and $^{1}J_{DN}$ for cytidine and thymidine, respectively. If these coupling constants were proportional to the gyromagnetic ratio, then ca. 0.4 and 13 Hz would be expected for $^{1h}J_{DN}$ and $^{1}J_{DN}$ from $^{1h}J_{HN}$ and $^{1}J_{HN}$, respectively. Actually, the magnitude of $^{1h}J_{DN}$ was small as compared to the linewidth, as judged from Figure 2. Another feature was the linewidth of the ^{15}N signals, in that the ^{15}N linewidths in D_2O with deuterium decoupling (Figure 2, c and f) were narrower than those in H_2O (Figure 2, a and d). The magnitude of the dipolar interaction between deuteron and nitrogen is smaller than that of a proton, and the scalar relaxation contribution from deuterium can be removed by the deuterium decoupling. These factors

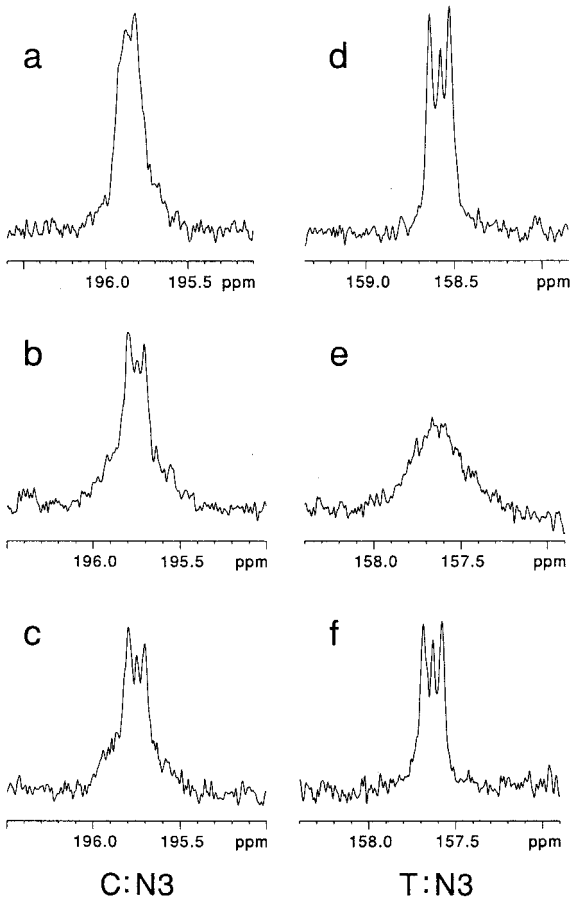

Figure 2. N3 signals of dC (a–c) and T (d–f) of d(CGC**GA**AT**TC**GCG)$_2$, recorded at 14.1 T at 35 °C in H_2O (a, d) and in D_2O, without (b, e) and with (c, f) deuterium decoupling.

explain the apparent sharpening of the ^{15}N signals in D_2O, as shown at the bottom of Figure 2 (c, f).

A systematic decrease of the $^{2h}J_{NN}$ value was found by elevating the temperature, as shown in Tables 1–3. It did not depend on the other physical and sample properties, i.e., the magnetic field strength, the DNA sequence, or the solvent. This temperature dependence was significant. For example, in Table 2 the $^{2h}J_{NN}$ values of the two A-tract samples decreased by 0.8 and 0.6 Hz by changing the temperature from 10 to 40 °C. It was also examined using the quantitative HNN-COSY method, as shown in Figure 3. In Figure 3, the open and filled circles indicate the AT and GC base pairs, respectively, and the error bars are given at 293 K. The determined $^{2h}J_{NN}$ values from the quantitative HNN-COSY method were systematically smaller than those from the splitting

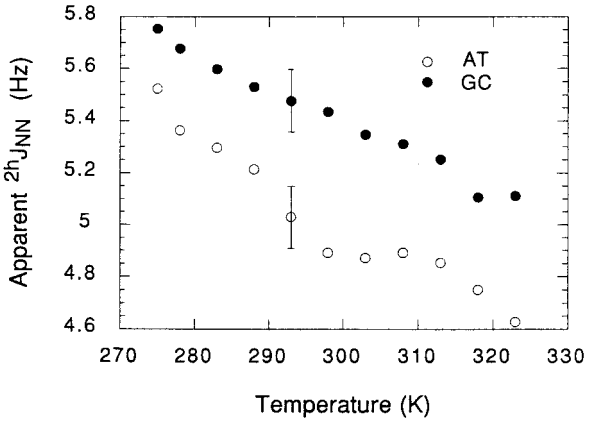

Figure 3. Temperature dependence of the apparent $^{2h}J_{NN}$ value of d(CGC**GA**AT**TC**GCG)$_2$, determined from quantitative HNN-COSY experiments at 14.1 T. The ^{15}N carrier frequency and the RF field strength are 185 ppm and 6.6 kHz, respectively. The open and closed circles are the AT and GC base pairs, respectively. The experimental error bars are given at 293 K. The ^{15}N concentration contribution and the insufficient ^{15}N RF power are not corrected.

Table 4. Ammonium effect of apparent ^{15}N-^{15}N J-couplings across the hydrogen bond[a]

Concentration NH_3 (mM)		Coupling at a temperature of 2 °C	20 °C	40 °C
0	AT	5.5	5.0 (6.8)	4.9
20	AT	5.4	5.2 (6.9)	n.d.
0	GC	5.8	5.5	5.3
20	GC	5.8	5.5	5.1

[a]Apparent $^{2h}J_{NN}$ (in Hz) between 5A(4G):N1 and 8T(9C):N3 for the AT(GC) base pair of d(CGC**GA**AT**TC**GCG)$_2$ in H_2O at 14.1 T obtained from quantitative HNN-COSY experiments. ^{15}N carrier frequency and RF field strength are 185 ppm and 6.6 kHz, respectively. The solution conditions were 10 mM sodium-phosphate buffer with 100 mM sodium chloride and 0.1 mM EDTA (pH 8.7). The NH_3 concentration, 0 or 20 mM, is given in the table. n.d.: Not determined due to broadening. In parentheses, the $^{2h}J_{NN}$ values obtained from the ^{15}N 1D splitting at 18.8 T are shown.

of the ^{15}N 1D spectrum. This systematic difference is discussed later in detail. In Figure 3, a significant decrease of $^{2h}J_{NN}$ was seen for both the AT and GC base pairs at the higher temperature. The temperature dependent decrease of $^{2h}J_{NN}$ can be understood in many ways, for example, by the physical decrease of the hydrogen bond strength by increasing the NN distance and/or decreasing the NH distance, and by the shift of the equilibrium between the open and closed states of the base pair toward the open state. Since the imino resonance comes from the closed state, but not the opened one, the second explanation seems less probable than the first. One of the other potential sources of the apparent decrease of $^{2h}J_{NN}$ was the exchange process between the imino proton and water. This proton exchange contribution was examined for a DNA dodecamer sample by adding 20 mM NH_3 at pH 8.7, as shown in Table 4. This NH_3 addition technique enhances the proton exchange with water (Leroy et al., 1988). The result was remarkable, in that there was no significant difference with and without 20 mM NH_3, although the apparent linewidth of each imino proton signal significantly broadened with NH_3. Dingley et al. pointed out that these increased exchange contributions will not affect the determined $^{2h}J_{NN}$ value in the quantitative HNN-COSY method (Dingley et al., 1999). Here our results confirmed this using 20 mM NH_3, and additionally confirmed that such an increased exchange contribution did not affect the splitting of the ^{15}N 1D signal.

Discussion

In the nucleic acid NMR field, there was a general question as to why the relatively large $^{2h}J_{NN}$ ($\sim$ 7 Hz) had not been found for such a long time. The most logical reason was the presence of the homonuclear ^{15}N-^{15}N coupling constants within the base ring and the relatively large ^{15}N linewidth of the oligomer, as mentioned in the Introduction. Here, these contributions on the apparent ^{15}N line shape were simulated using the apparent ^{15}N linewidth of our DNA dodecamer, 3.8 Hz at 20 °C and 14.1 T in H_2O. The homonuclear ^{15}N-^{15}N coupling constants within the base rings of adenosine, guanosine, cytidine, and thymidine were obtained from the literature (Levy and Lichter, 1979; Ono, 1997; Dingley et al., 1999). The $^{2h}J_{NN}$ values were assumed to be 5.9 and 6.9 Hz for the GC and AT base pairs, respectively. The simulated spectra are shown in Figure 4. The bottom (e–h) and top (a–d) spectra were simulated with and without $^{2h}J_{NN}$, respectively. The contribution of $^{2h}J_{NN}$ is clearly seen by comparing the top (a–d) to the bottom (e–h) in Figure 4, and it seemed to be possible to determine the quantitative values of $^{2h}J_{NN}$. Consequently, the reason why the large $^{2h}J_{NN}$ had not been found was neither the presence of the homonuclear ^{15}N-^{15}N cou-

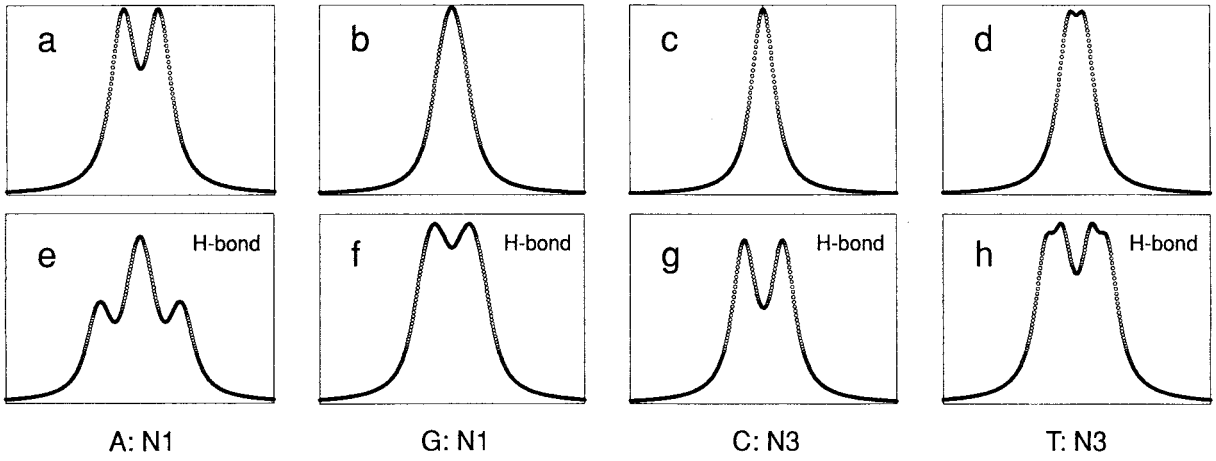

Figure 4. Simulated $^{15}N\{^{1}H\}$ 1D spectrum without (a–d) and with $^{2h}J_{NN}$ contributions (e–h) for adenosine N1 (a, e), guanosine N1 (b, f), cytidine N3 (c, g), and thymidine N3 (d, h), from the left side to the right. The homonuclear ^{15}N-^{15}N coupling constants and the ^{15}N linewidth were obtained from the literature and our experimental results.

pling constants within the base ring nor the relatively large ^{15}N linewidth of the oligomer, although it was generally believed that the relatively large ^{15}N-^{15}N coupling constants were present within the base ring, and not across the hydrogen bond. The quantitative determination of $^{2h}J_{NN}$ was actually possible by reading the ^{15}N splitting of uniformly ^{15}N or $^{13}C/^{15}N$ labeled samples, as demonstrated by Pervushin et al. (1998, 2000), but a highly quantitative determination of the ^{15}N splitting did not seem to be easy, as judged from the simulated results shown in Figure 4. The merit of the N3 atom-specific labeling is clear when comparing the simulated spectra in Figure 4 to the observed spectra in Figure 1. Especially, the N3 signal of thymidine was sharpened, due to the absence of the homonuclear 2.6 Hz ^{15}N-^{15}N coupling within the base ring. Thus, the direct reading of the splitting, as demonstrated in this report, will not give quantitative $^{2h}J_{NN}$ values for uniformly ^{15}N or $^{13}C/^{15}N$ labeled samples.

The $^{2h}J_{NN}$ values determined from the quantitative HNN-COSY method were systematically smaller than those from the splitting of the ^{15}N 1D spectrum, as described above. For example, the $^{2h}J_{NN}$ values of the AT base pair at 20 °C were 5.0 and 7.0 Hz by the quantitative HNN-COSY and ^{15}N 1D methods, respectively (see Tables 1 and 4). These values should be identical within the experimental errors. There were several possibilities to explain the difference, such as the lower ^{15}N fraction of our samples, the insufficient ^{15}N RF power, the linewidth differences between the purine N1 and pyrimidine N3 signals, and so on. The first ^{15}N fraction contribution in the quantitative HNN-COSY experiment was theoretically treated to correct the relative intensity of the diagonal and the cross peak. If the ^{15}N fraction was 100%, then the intensity ratio of the cross to diagonal peaks would be given as follows:

$$I_c/I_d = \tan^2(2\pi J_{NN}T) \quad (1)$$

where I_c and I_d are the intensities of the cross and diagonal peaks, and J_{NN} and T are the J coupling constants and the delay time used for the ^{15}N to ^{15}N coherence transfer. In the quantitative HNN-COSY experiment, the thymidine N3 and guanosine N1 signals were used for the final detection via the imino proton. Thus, their ^{15}N fractions were not affected by the I_c/I_d ratio. The J_{NN} modulated fraction of the diagonal peak as well as the cross peak was simply identical to the ^{15}N fraction of the base paired nitrogen, i.e., adenosine N1 and cytidine N3. When the ^{15}N fractions of adenosine N1 and cytidine N3 were defined as α, Equation 1 was modified as follows:

$$I_c/I_d = [\alpha \times \sin^2(2\pi J_{NN}T)]/[(1-\alpha)+\alpha \times \cos^2(2\pi J_{NN}T)] \quad (2)$$

where the difference of the relaxation times between the $^{15}N \bullet {}^{1}H$–^{15}N and $^{14}N \bullet {}^{1}H$–^{15}N systems was not considered. Using the ^{15}N fractions of adenosine N1 and cytidine N3 (79 and 88%, respectively), Equation 2 was applied to correct the determined $^{2h}J_{NN}$ value. A 10 to 15% increase of the apparent $^{2h}J_{NN}$ was obtained by this ^{15}N fraction contribution correction; however, the observed difference of ∼ 40% was not explained completely.

Table 5. Comparison of $^{2h}J_{NN}$ values obtained from HNN-COSY and ^{15}N splitting[a]

Technique	Coupling (Hz)
HNN-COSY	5.0
HNN-COSY with composite 180° pulses	5.7
HNN-COSY with ^{15}N concentration correction	5.8
HNN-COSY with both corrections	6.6
^{15}N splitting	7.0

[a] $^{2h}J_{NN}$ (in Hz) between 5A:N1 and 8T:N3 of d(CGCG**A**AT**T**CGCG)$_2$ in H_2O at 14.1 T and 20 °C obtained from quantitative HNN-COSY experiments (first row), quantitative HNN-COSY with composite 180° pulses (second), with ^{15}N concentration correction (third), with both corrections (forth), and ^{15}N splitting (last row). ^{15}N carrier frequency and RF field strength are 185 ppm and 6.6 kHz, respectively.

The insufficient ^{15}N RF power contribution was corrected experimentally. The two 180 °C pulses used for the ^{15}N to ^{15}N coherence transfer were replaced with 90°-270°-90° composite pulses. The obtained $^{2h}J_{NN}$ values with the ^{15}N fraction contribution correction, with the composite pulses, and with both corrections are given in Table 5. The insufficient ^{15}N RF power contribution of the $^{2h}J_{NN}$ value underestimation, 10–15%, is comparable to that of the lower ^{15}N fraction of our samples. The $^{2h}J_{NN}$ value in which both effects are corrected is about 5% smaller than that of the ^{15}N 1D method. This difference may come from the imperfection of the other ^{15}N pulses, which can be eliminated by using soft-HNN-COSY based spin-echo difference techniques (Majumdar et al., 1999a; Dingley et al., 2000). Compared to the initial difference of $\sim$ 40%, the apparent $^{2h}J_{NN}$ value was almost recovered by these corrections.

The N1 to N3 linewidth difference contribution was briefly mentioned by Dingley and Grzesiek (1998), and the peak area integration, not the peak height, was recommended to calculate the I_c / I_d ratios. Therefore, the peak area integration was employed here. Moreover, our point resolution in t_1 was two to four times higher than that of Dingley and Grzesiek. Our samples were smaller than those of Grzesiek's group (Dingley and Grzesiek, 1998; Dingley et al., 1999), and thus the point resolution could still be the problem. To determine the point resolution contribution, two independent experiments using two different point resolutions, 5 and 10 Hz per point in t_1, were performed, but no significant difference was found. Consequently, the difference of the $^{2h}J_{NN}$ values obtained from the quantitative HNN-COSY and ^{15}N 1D methods was due to the insufficient ^{15}N RF power in the quantitative HNN-COSY experiment and the lower ^{15}N fraction of our samples. This difference was almost recovered by the theoretical correction of the ^{15}N fraction contribution and by the experimental replacement of the ^{15}N 180° pulses with the 90°-270°-90° composite pulses.

For the Watson–Crick AT and GC base pairs of the DNA duplex, the $^{2h}J_{NN}$ values were reported in the 6.0 to 7.0 Hz range (Pervushin et al., 1998, 2000). For those of the DNA triplex, the $^{2h}J_{NN}$ values were 8.5 ± 0.4 Hz and 6.6 ± 0.6 Hz for AT and GC, respectively (Dingley et al., 1999). In our case, they were in the 6.5 to 7.6 Hz range for AT (Tables 1–3), consistent with the results of Pervushin et al. (1998, 2000). As compared to the results of Dingley et al. (1999), the $^{2h}J_{NN}$ value of the GC base pair was not different, but for the AT base pairs it was completely different from ours and others (Pervushin et al., 1998, 2000). As examined in this report, the $^{2h}J_{NN}$ values depended on the temperature and the ^{15}N RF pulse power. However, these factors are not sufficient to explain it. The most reasonable explanation is the difference of the sample, e.g., the shorter distance between the two base paired nitrogens and/or the longer N–H bond length, which are specific for a DNA triplex.

For the Watson–Crick AU base pairs of RNA, the $^{2h}J_{NN}$ values were reported as 6.7 ± 0.5 Hz by Dingley and Grzesiek (1998). We determined the $^{2h}J_{NN}$ value for the AU base pair of DNA as 7.3 Hz at 20 °C by the ^{15}N 1D method (Kojima et al., unpublished results), which is slightly larger. The ^{15}N RF power of 5.9 kHz used in their first report (Dingley and Grzesiek, 1998) did not seem to be sufficient for quantitative HNN-COSY experiments, and the obtained J values were uniformly underestimated by 10–15%, as suggested in their reports (Dingley and Grzesiek, 1998; Dingley et al., 1999). If this underestimation is taken into account, then our results are in good agreement with the previous report (Dingley and Grzesiek, 1998).

Conclusions

The N3-site selectively ^{15}N enriched pyrimidine nucleotides were prepared to study the scalar coupling constants across the hydrogen bond ($^{2h}J_{NN}$). The purine nucleotides were uniformly ^{15}N enriched and were incorporated into the DNA oligomer site-specifically with ^{15}N enriched pyrimidine nucleotides. This selective labeling technique enabled us to determine the $^{2h}J_{NN}$ value from the splitting of the ^{15}N 1D

spectrum (Figure 1). The ^{15}N fractions of our samples were 79 and 88% for dA and the other nucleotides, respectively, which were sufficient to see the signals, but the resultant $^{2h}J_{NN}$ values were seriously affected by such small imperfections in the ^{15}N enrichment. The center peak contribution was carefully treated using the line shape fitting tool of the FELIX software. The determined $^{2h}J_{NN}$ values, 6.5 to 7.6 Hz for the AT base pair, were consistent with those of previous reports.

Three or four different temperatures between 10 and 50 °C were used to see the temperature dependence of $^{2h}J_{NN}$ and to assess the magnetic field dependence (Table 1), the DNA sequence dependence (Table 2), and the solvent dependence (Table 3). No significant dependence was found on the magnetic field strength and the DNA sequence. On the other hand, in D_2O the $^{2h}J_{NN}$ values were 0.3–0.4 Hz smaller than those in H_2O. A systematic decrease of $^{2h}J_{NN}$ was found by elevating the temperature (Tables 1–3, Figure 3). This temperature dependent decrease was not due to the imino proton–water exchange process, since the addition of 20 mM NH_3 did not affect $^{2h}J_{NN}$ (Table 4). The $^{2h}J_{NN}$ values determined by the quantitative HNN-COSY method were systematically smaller than those from the splitting of the ^{15}N 1D spectrum (Tables 1–4, Figure 3). These differences were due to the insufficient ^{15}N RF power in the quantitative HNN-COSY experiment and the lower ^{15}N fraction of our samples, and they were almost completely recovered by the theoretical correction of the ^{15}N fraction contribution using Equation 2 and the experimental replacement of the ^{15}N 180° pulses with 90°-270°-90° composite pulses (Table 5).

Acknowledgements

We thank Drs. Stephan Grzesiek and John L. Markley for helpful discussions. This work was supported by CREST (Core Research for Evolutional Science and Technology) of the Japan Science and Technology Cooperation (JST) and by a Grant-in-Aid for Scientific Research on Priority Areas from the Ministry of Education, Science and Culture (09235237).

References

Ariza, X., Bou, V. and Vilarrasa, J. (1995) *J. Am. Chem. Soc.*, **117**, 3665–3673.

Benedict, H., Limbach, H.-H., Wehlan, M., Fehlhammer, W.-P., Golubev, N.S. and Janoschek, R. (1998) *J. Am. Chem. Soc.*, **120**, 2939–2950.

Cordier, F. and Grzesiek, S. (1999) *J. Am. Chem. Soc.*, **121**, 1601–1602.

Cornilescu, G., Hu, J.-S. and Bax, A. (1999) *J. Am. Chem. Soc.*, **121**, 2949–2950.

Dingley, A.J. and Grzesiek, S. (1998) *J. Am. Chem. Soc.*, **120**, 8293–8297.

Dingley, A.J., Masse, J.E., Peterson, R.D., Barfield, M., Feigon, J. and Grzesiek, S. (1999) *J. Am. Chem. Soc.*, **121**, 6019–6027.

Dingley, A.J., Masse, J.E., Feigon, J. and Grzesiek, S. (2000) *J. Biomol. NMR*, **16**, 279–289.

Hennig, M. and Geierstanger, B.H. (1999) *J. Am. Chem. Soc.*, **121**, 5123–5126.

Hennig, M. and Williamson, J.R. (2000) *Nucleic Acids Res.*, **28**, 1585–1593.

Hibbert, F. and Emsley, J. (1990) *Adv. Phys. Org. Chem.*, **26**, 255–379.

Kyogoku, Y., Kojima, C., Lee, S.J., Tochio, H., Suzuki, N., Matsuo, H. and Shirakawa, M. (1995) *Methods Enzymol.*, **261**, 524–541.

Leroy, J.-L., Charretier, E., Kochoyan, M. and Guéron, M. (1988) *Biochemistry*, **27**, 8894–8898.

Levy, G.C. and Lichter, R.L. (1979) *Nitrogen-15 Nuclear Magnetic Resonance Spectroscopy*, John Wiley & Sons, Inc., New York, NY.

Liu, A., Majumdar, A., Hu, W., Kettani, A., Skripkin, E. and Patel, D.J. (2000) *J. Am. Chem. Soc.*, **122**, 3206–3210.

Majumdar, A., Kettani, A. and Skripkin, E. (1999a) *J. Biomol. NMR*, **14**, 67–70.

Majumdar, A., Kettani, A., Skripkin, E. and Patel, D.J. (1999b) *J. Biomol. NMR*, **15**, 207–211.

Ono, A., Tate, S. and Kainosho, M. (1994) In *Stable Isotope Application in Biomolecular Structure and Mechanisms* (Eds, Trewhella, J., Cross, T.A. and Unkefer, C.J.), Los Alamos National Laboratory, Los Alamos, NM, pp. 127–144.

Ono, M.A. (1997) Doctoral thesis, Tokyo Metropolitan University, Tokyo.

Pervushin, K., Ono, A., Fernández, C., Szyperski, T., Kainosho, M. and Wüthrich, K. (1998) *Proc. Natl. Acad. Sci. USA*, **95**, 14147–14151.

Pervushin, K., Fernández, C., Riek, R., Ono, A., Kainosho, M. and Wüthrich, K. (2000) *J. Biomol. NMR*, **16**, 39–46.

Scheurer, C. and Brüschweiler, R. (1999) *J. Am. Chem. Soc.*, **121**, 8661–8662.

Wöhnert, J., Dingley, A.J., Stoldt, M., Görlach, M., Grzesiek, S. and Brown, L.R. (1999) *Nucleic Acids Res.*, **27**, 3104–3110.